Neuropharmacology 229 (2023) 109481

Contents lists available at ScienceDirect

Neuropharmacology

journal homepage: www.elsevier.com/locate/neuropharm

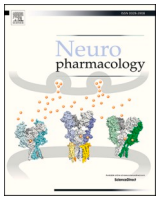

Ketamine reduces electrophysiological network activity in cortical neuron cultures already at sub-micromolar concentrations – Impact on TrkB-ERK1/2 signaling

A. Ahtiainen [a,**,1], I. Annala [b,c,1,*], M. Rosenholm [b,d], S. Kohtala [b,c,e], J. Hyttinen [a], J.M.A. Tanskanen [a], T. Rantamäki [b,c]

[a] Computational Biophysics and Imaging Group, BioMediTech, Faculty of Medicine and Health Technology, Tampere University, Arvo Ylpön katu 34, 33520, Tampere, Finland
[b] Laboratory of Neurotherapeutics, Drug Research Program, Division of Pharmacology and Pharmacotherapy, Faculty of Pharmacy, University of Helsinki, Viikinkaari 5E, Biocenter 2, 00790, Helsinki, Finland
[c] SleepWell Research Program, Faculty of Medicine, University of Helsinki, P.O. Box 9, Helsinki, 00014, Finland
[d] Center for Translational Neuromedicine, Faculty of Health and Medical Sciences, University of Copenhagen, Blegdamsvej 3B, 2200, Copenhagen N, Denmark
[e] Department of Psychiatry, Feil Family Brain and Mind Research Institute, Weill Cornell Medicine, 407 E 61st St, New York, NY, 10065, USA

ARTICLE INFO

Keywords:
Ketamine
Extracellular electrophysiology
Microelectrode array
Cortical neuron culture
Neuronal activity
TrkB phosphorylation

ABSTRACT

The dissociative anesthetic ketamine regulates cortical activity in a dose-dependent manner. Subanesthetic-dose ketamine has paradoxical excitatory effects which is proposed to facilitate brain-derived neurotrophic factor (BDNF) (a ligand of tropomyosin receptor kinase B, TrkB) signaling, and activation of extracellular signal-regulated kinase 1/2 (ERK1/2). Previous data suggests that ketamine, at sub-micromolar concentrations, induces glutamatergic activity, BDNF release, and activation of ERK1/2 also on primary cortical neurons. We combined western blot analysis with multiwell-microelectrode array (mw-MEA) measurements to examine ketamine's concentration-dependent effects on network-level electrophysiological responses and TrkB-ERK1/2 phosphorylation in rat cortical cultures at 14 days *in vitro*. Ketamine did not cause an increase in neuronal network activity at sub-micromolar concentrations, but instead a decrease in spiking that was evident already at 500 nM concentration. TrkB phosphorylation was unaffected by the low concentrations, although BDNF elicited prominent phosphorylation response. High concentration of ketamine (10 μM) strongly reduced spiking, bursting and burst duration, which was accompanied with decreased phosphorylation of ERK1/2 but not TrkB. Notably, robust increases in spiking and bursting activity could be produced with carbachol, while it did not affect phosphorylation of TrkB or ERK1/2. Diazepam abolished neuronal activity, which was accompanied by reduced ERK1/2 phosphorylation without change on TrkB. In conclusion, sub-micromolar ketamine concentrations did not cause an increase in neuronal network activity or TrkB-ERK1/2 phosphorylation in cortical neuron cultures that readily respond to exogenously applied BDNF. Instead, pharmacological inhibition of network activity can be readily observed with high concentration of ketamine and it is associated with reduced ERK1/2 phosphorylation.

This article is part of the Special Issue on "Ketamine and its Metabolites".

1. Introduction

Ketamine is an N-methyl-D-aspartate receptor (NMDAR) antagonist with a variety of clinical uses spanning from anesthesia to pain management and treatment of depression (Zanos et al., 2018). Besides racemic ketamine – 1:1 mixture of (S)- and (R)-enantiomers – also

* Corresponding author. Laboratory of Neurotherapeutics, Drug Research Program, Division of Pharmacology and Pharmacotherapy, Faculty of Pharmacy, University of Helsinki, Viikinkaari 5E, Biocenter 2, 00790, Helsinki, Finland.
** Corresponding author.
E-mail addresses: annika.ahtiainen@tuni.fi (A. Ahtiainen), iina.annala@helsinki.fi (I. Annala).
[1] Equal Contribution.

https://doi.org/10.1016/j.neuropharm.2023.109481
Received 5 February 2023; Received in revised form 24 February 2023; Accepted 26 February 2023
Available online 2 March 2023

(S)-ketamine (Zanos et al., 2018), and possibly (R)-ketamine (Leal et al., 2021), alone produce antidepressant effects in humans. Patients with major depression typically experience rapid relief of depressive symptoms following the administration of subanesthetic doses of ketamine (Marcantoni et al., 2020), the mechanism of which has been a subject of intense study.

Subanesthetic ketamine causes acute increases in electroencephalography gamma power, which is suggested to be a biomarker of cortical activation (de la Salle et al., 2016; Muthukumaraswamy et al., 2015; Zanos et al., 2016; Kohtala et al., 2019b). Subanesthetic-dose ketamine has also been shown to increase extracellular glutamate levels in the prefrontal cortex in adult rodents, whereas anesthetic doses decrease glutamate release (Moghaddam et al., 1997). This peculiar dose-response profile has been explained by ketamine's preference to block NMDARs in gamma-aminobutyric acid-releasing (GABAergic) inhibitory interneurons at low doses, leading to disinhibition of pyramidal neurons and glutamate bursting (Ali et al., 2020; Gerhard et al., 2020; Homayoun and Moghaddam, 2007). The facilitation of neuronal activity and glutamate release is then proposed to trigger α-amino-3--hydroxy-5-methyl-4-isoxazolepropionic acid receptor (AMPAR)-dependent cascades of biochemical events at the postsynaptic side, leading to facilitation of neuronal plasticity and antidepressant effects (Li et al., 2010).

Brain-derived neurotrophic factor (BDNF) has been strongly connected to antidepressant effects (Castrén et al., 2007; Duman et al., 2021). BDNF signaling plays a key role in the formation of neuronal networks during early development and continues to be important for neuronal plasticity in the mature nervous system (Park and Poo, 2013). Importantly, the expression and release of BDNF is under activity-dependent regulation (Miyasaka and Yamamoto, 2021; Thoenen, 1995). Upon BDNF binding, the cognate receptor tropomyosin receptor kinase B (TrkB) dimerizes and undergoes autophosphorylation, initiating intracellular signaling cascades that include extracellular signal-regulated kinases 1 and 2 (ERK1/2), Akt and phospholipase Cγ (PLCγ) pathways (Park and Poo, 2013). Notably, ketamine's antidepressant effects have been mechanistically connected to increased signaling of both TrkB and ERK1/2 (Lepack et al., 2015; Li et al., 2010; Liu et al., 2012; Yang et al., 2015). The subanesthetic doses of ketamine upregulate, while anesthetic doses downregulate, ERK1/2 signaling in the adult rodent prefrontal cortex (Kohtala et al., 2019a, 2019b; Li et al., 2010; Salort et al., 2019), which is suggested to be dependent on neuronal activity (Li et al., 2010). Yet, ketamine has also been hypothesized to affect the BDNF-TrkB signaling independently of neuronal activation through induction of local BDNF synthesis (Autry et al., 2011; Nosyreva et al., 2013) or more recently, through direct binding to TrkB (Casarotto et al., 2021). Moreover, we have recently shown that anesthetic doses of ketamine activate TrkB in the cortex more efficiently compared to subanesthetic doses (Kohtala et al., 2019a), further underlining the open questions around the relationship between cortical activity, TrkB signaling and antidepressant effects of ketamine (Kohtala, 2021; Kohtala and Rantamäki, 2021).

The effects of ketamine have also been studied in primary rat cortical neuronal cultures, where low micromolar concentrations were reported to induce BDNF release and ERK phosphorylation (Lepack et al., 2015, 2016). These effects could be blocked by an AMPAR antagonist, favoring the activity-dependent mechanism, and suggesting that the network-level effects could be recapitulated in dissociated neuron cultures. However, the electrophysiological activity or activation of TrkB were not directly measured in these studies. To this end, we have here examined the concentration-dependent effects of ketamine on neuronal network activity in primary rat cortical neuron cultures by using multiwell-format microelectrode array (mw-MEA) platform. This method allows exploration of network-level electrophysiological activity of cultures noninvasively by measuring the activity with multiple extracellular electrodes simultaneously (Thomas et al., 1972; Wagenaar et al., 2006a; Ylä-Outinen et al., 2019). We combined the measurement of MEA activity with assessment of TrkB and ERK1/2 phosphorylation to elucidate the relationship between neuronal activity and BDNF signaling *in vitro*.

2. Materials and methods

2.1. Multiwell MEA plates

Sterile and sealed twenty-four-well Multiwell-MEA-plates (24W300/30G-288, Multi Channel Systems MCS GmbH, Reutlingen, Germany) comprising of 12 planar poly 3,4-ethylene-dioxythiophene (PEDOT)-coated gold electrodes in 4 x 4 grid (electrode spacing 300 μm and diameter 30 μm) in each well were coated and incubated with 0.1 mg/ml poly-D-lysine (PDL, Sigma-Aldrich, St. Louis, MO, USA) for 1 h. Wells were washed three times with Milli-Q water, air dried in laminar hood, and incubated with laminin (L2020, 20 μg/ml in DPBS, Sigma-Aldrich, St. Louis, MO, USA) for 2 h at +37 °C or alternatively overnight at +4 °C. Excess laminin was removed just before plating the cells.

2.2. Primary cortical cultures

Frozen and cryoprotected E18 primary rat cortical neurons (A1084001, Thermo Fisher Scientific, Waltham, MA, USA) were thawed, centrifuged at 250×*g* for 3–4 min and resuspended in fresh pre-warmed culture medium containing Neurobasal™ Plus medium with 2% B-12 Plus supplement, 1% Penicillin-Streptomycin (P/S), and 0.25% GlutaMAX supplement (all purchased from Thermo Fisher Scientific, Waltham, MA, USA). Cell number and viability were determined using Countess Automated Cell Counter (Thermo Fisher Scientific, Waltham, MA, USA), and approximately 80,000 neurons were seeded per each mw-MEA well. High cell densities were used for MEA experiments to allow adequate protein concentration for immunoblot analysis needed in protein assays. Neurons were also plated on PDL/L2020 treated glass coverslips for immunocytochemical staining. Cells were maintained in a 5% CO_2 humidified incubator at +37 °C. Half of the cell medium was replaced to fresh pre-warmed culture medium every two to three days, and always after electrophysiological recordings.

2.3. Immunocytochemical staining

To understand the basic cellular composition and characteristics of the cultures, we performed immunocytochemical stainings (ICC). Cells were washed with Dulbecco's phosphate-buffered saline (D-PBS, Thermo Fisher Scientific, Waltham, MA, USA) and subsequently fixed using 3.7% paraformaldehyde (Sigma-Aldrich, St. Louis, MO, USA) in PBS for 20 min at room temperature (RT). Cells were permeabilized with 0.3% Triton X-100 (Sigma-Aldrich, St. Louis, MO, USA) in PBS for 10 min at RT and subsequently blocked with 5% (v/v) goat serum (GS; GS, Sigma–Aldrich, St. Louis, MO, USA) in PBS for 2 h at RT. Primary antibodies were diluted to 5% (v/v) GS-PBS and incubated overnight at +4 °C. Primary antibodies were neuron-specific βIII-tubulin (β3tub; MA1-118, mouse, 1:1000), Glial Fibrillary Acidic Protein (GFAP; MA5-12023, mouse, 1:1000 or PA1-10004, chicken, 1:1000), Microtubule Associated Protein 2 (MAP-2; PA1-10005, chicken, 1:1000 or MAB3418, mouse, 1:1000), S100β (PA5-78161; rabbit, 1:500), Synaptophysin (SYN; MA5-14532; rabbit, 1:500) and gamma-aminobutyric acid (GABA; PA5-32241; rabbit, 1:500). The next day, cells were rinsed three times with 0.1% Triton X-100 in PBS and incubated in the dark for 1 h at RT with species-specific Alexa Fluor conjugated secondary antibodies (A-11001, A32933 and A-21428; 1:500) diluted to 5% (v/v) GS-PBS. All antibodies, except MAB3418 (Sigma-Aldrich, St. Louis, MO, USA), were purchased from Thermo Fisher Scientific (Waltham, MA, USA). Next, cells were washed twice with 0.1% Triton X-100 in PBS, followed by 1:1000 addition of nuclei label 4′,6-diamidino-2-phenylindole (DAPI; D1306, 10 μg/ml in PBS, Thermo Fisher Scientific, Waltham, MA, USA) for 10 min at RT. Samples were rinsed with PBS, after which coverslips

were mounted onto microscope glasses using ProLong™ Gold Antifade Mountant (P36930, Thermo Fisher Scientific) and cured for 24 h in the dark at RT. Coverslips were stored at +4 °C until imaged with Olympus IX51 Fluorescence Microscope (Olympus Corporation, Hamburg, Germany) or with Nikon Eclipse Ti2 (Nikon Instruments, Inc., Melville, NY, USA) fluorescent microscope with an ORCA-Fusion camera (model: C14440–20UP, Hamamatsu Photonics K. K., Hamamatsu City, Japan) for the GABA staining. Images were then further processed using Fiji (ImageJ, National Institute of Health, USA) software.

2.4. Pharmacological treatments

Ketamine hydrochloride (Yliopiston Apteekki, Finland), recombinant BDNF (Peprotech, #450-02), diazepam (Sigma, #D0899) and carbachol (carbamoylcholine chloride; Tocris, #2710) were used for pharmacological stimulations. The stock solutions (100 μM-10 mM for ketamine; 20 μg/ml for BDNF; 10 mM for diazepam; 25 mM for carbachol) were prepared in PBS, except for diazepam that was prepared in 10% dimethyl sulfoxide (DMSO) in PBS. Stimulations were performed on 14 or 35 days *in vitro* (DIV) mature cultures grown on mw-MEA plates. Each experiment had their respective control wells on the same plate (n = 6–8). Control treatment in all experiments was PBS. The chemicals or control solutions were added into wells by pipetting 1 μl of the stock solution or PBS directly to the cell culture medium (volume = 1 ml), resulting in the final concentrations of 100 nM, 250 nM, 500 nM or 10 μM (ketamine), 20 ng/ml (BDNF), 10 μM (diazepam) and 25 μM (carbachol) (n = 6–8 in each group). In the case of diazepam, the final DMSO concentration was 0.01%. Each culture was treated with only one drug before lysis, except diazepam was added on top of carbachol.

2.5. Microelectrode array recordings and electrophysiological data analysis

The cultures were let to adapt for at least 5 min before recording. For characterization of activity over *in vitro* development, spontaneous activity of one plate (n = 24) was measured from DIV4 until DIV35 three times a week for 5 min. For studying the effects of treatments, spontaneous baseline activity was first recorded for 5 min. After establishing the baseline, the compounds or control solutions were added to the media and the recording of treatment period was started. In case of BDNF and ketamine studies, the recording period was 15 min. The recording time in carbachol and diazepam experiment was 30 min: a subset of the cultures were exposed to carbachol for the whole 30-min recording, whereas another set of carbachol-containing wells were applied diazepam for the last 15 min of the recording. All recordings were maintained at +37 °C and 5% CO_2 atmosphere.

Signals were recorded and analyzed with Multiwell-Screen and Multiwell-Analyzer -softwares (Multichannel Systems MCS GmbH, Reutlingen, Germany) and Matlab R2021b (MathWorks, Inc., Natick, MA, USA) with 20 kHz sampling rate. Recordings were then high-pass filtered at 200 Hz a. A threshold-based detector of ±5.0x estimated noise was used for spike detection. A burst was considered as four or more spikes and an interspike interval (ISI) under 100 ms. Most of the used burst specifications, i.e., the maximum interspike interval in bursts, were selected as they are widely used in the MEA field (e.g., Hyvärinen et al., 2019; Wagenaar et al., 2006a,b).

Culture wells containing at least four active electrodes during the baseline recording were included in the MEA and western blot (Section 2.6) analyses. In case of longitudinal recording of spontaneous activity, a well was excluded if it did not meet this criterion in any recording during the 35-day period. Electrode was considered active if it had ≥10 spikes/min. Only the electrodes that fulfilled this criterion during the analysis period in question (i.e., baseline or treatment period) were considered for the spike and burst analyses of that respective period – that is, the results per well represent average activity per active electrode, and the change in number of active electrodes is shown separately. The analyzed electrical activity parameters in this study were: spike rate (average number of spikes per minute); burst rate (average number of bursts per minute); burst duration (mean duration of a burst in milliseconds); spikes per burst (average number of spikes in a burst); spike rate in bursts (mean firing rate in bursts in Hz); % of spikes in bursts (average percentage of spikes that occur inside bursts); and interburst interval (average time period between consecutive bursts in seconds). A schematic representation of the used mw-MEA, its electrode layout, and some of the used spike and burst parameters are shown in Fig. 1. In ketamine and BDNF experiments, the activity during the entire 15-min treatment period was taken into the analyses. In the case of carbachol and diazepam experiment, we analyzed the activity during the 15–30 min period for all wells. In all experiments, the same time period was analyzed from the respective control wells. The activity during control or drug treatment was normalized to the baseline activity of the respective well. The change in activity from the baseline in the pharmacologically stimulated wells were compared to the respective average change in the control wells of the same plate.

In addition, we also quantified the level of burst synchronization during drug or respective control treatments. This was assessed by calculating the numbers of simultaneously occurring bursts based on individual burst information (burst start time, burst duration, and burst end time) for every mw-MEA well separately using an in-house MATLAB script. For each electrode data, a binary string was formed with 1s at the places of the measurement samples during bursts and 0s elsewhere. The binary data vectors of all electrodes in the mw-MEA well were summed, yielding a data vector indicating how many electrodes exhibited bursts at any time point. The maximum of the sum vector was taken to represent the level of simultaneous, or synchronized bursting of the network in the mw-MEA well; this maximum value was used in the statistical analysis and is shown in the related result plots. Due to the number of electrodes (12) in each mw-MEA well, the maximum value for simultaneous bursts is twelve, which means that at some time point(s) during the measurement, bursts were observed at all electrodes simultaneously in the mw-MEA well. Likewise, a value of one means that bursts occurred only at single electrode(s) at the time. This burst synchronization measure indicates the maximum spatial extent of simultaneous bursting activity in the network, and thusly is telling also of the maximum spatial bursting-related connectivity; such burst synchronization may to change due to pharmacological stimulation.

2.6. Western blot analysis

Immediately after the 15- or 30-min MEA-recording, we lysed the cultures directly on the mw-MEA wells. The plate was placed on top of ice and the drug-containing media was replaced with 75 μl lysis buffer containing phosphatase and protease inhibitors (137 mM NaCl, 20 mM Tris, 1% NP-40, 10% glycerol, 48 mM NaF, H2O, PierceTM Phosphatase and Protease Inhibitor tablets [Thermo Fisher Scientific]). After mechanical disruption, the samples corresponding to lysed cells from the individual cultures were collected and frozen (−80 °C). After thawing, the samples were centrifuged (16000×*g*, 15 min, +4 °C) and the resulting pellets discarded. The total protein concentrations of the supernatants were measured using DC™ protein assay kit (Bio-Rad Laboratories, Hercules, CA). Samples containing equal amounts of total protein (15–20 μg) were mixed in 1:1 ratio with 2x Laemmli Sample Buffer (Bio-Rad) supplemented with β-mercaptoethanol, heated in 100 °C for 3 min and then loaded to sodium dodecyl sulphate (SDS)–polyacrylamide gels (4–12% NuPAGE™, Thermo Fisher Scientific).The proteins were electrophoretically separated (180 V) under reducing and denaturing conditions, and then blotted to a polyvinylidene difluoride membrane as previously described (Kohtala et al., 2019b). Membranes were incubated with the following primary antibodies overnight: anti-phospho-TrkB^{Y816} (#4168; 1:1000; Cell signaling technology [CST]), anti-TrkB (#AF1494, 1:1000; R&D Systems) anti--phospho-ERK1/2$^{Thr202/Y204}$ (#9106 or #9101, 1:1000, CST) and

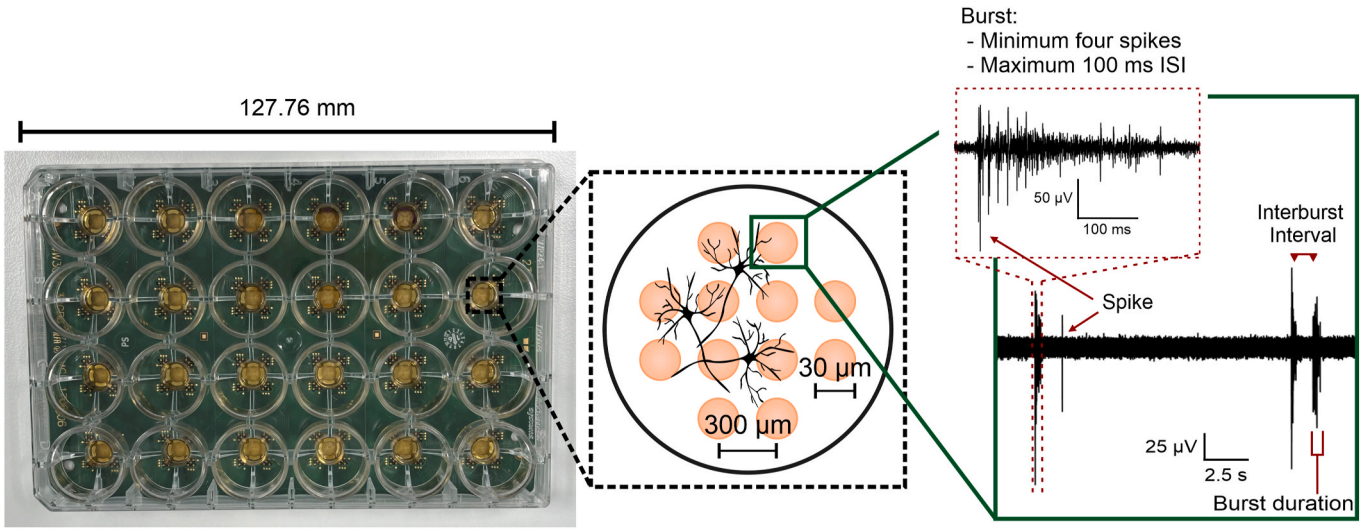

Fig. 1. Multiwell-MEA (mw-MEA) consists of 24 culture wells per plate. Twelve recording electrodes (indicated by orange circles) in the bottom of each well measure extracellularly the electrical activity of the neuronal networks growing on top of them. Neurons transmit signals as single spikes as well as rapid series of spikes, referred to as bursts. The image depicting neurons growing on top of electrodes is not in scale.

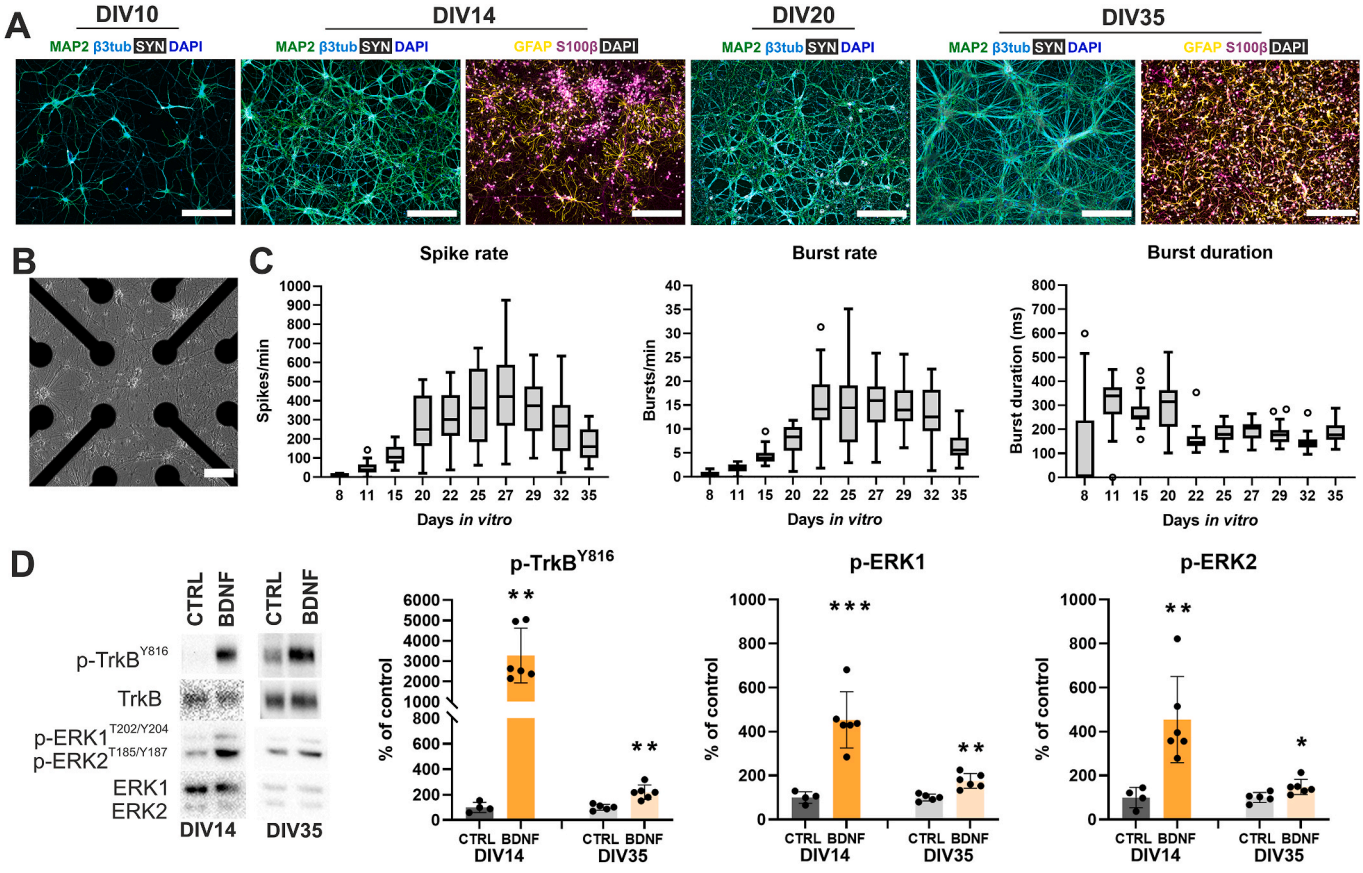

Fig. 2. Morphological and electrophysiological maturation and BDNF responses of neuronal networks formed by E18 rat cortical neurons. A) Immunocytochemical staining of a representative culture showing cortical neurons (MAP2 and βIII-tubulin), astrocytes (GFAP, S100β), and presynaptic proteins (synaptophysin [SYN]) from 10 to 35 days *in vitro* (DIV). The cell nucleus (DAPI) is indicated in blue for the neurons and white for the astrocytes. Scale bar is 200 µm. **B)** Phase-contrast image of DIV15 culture on mw-MEA. The scale represents 100 µm. **C)** The number of spikes and bursts per minute and burst duration in mw-MEA over development up to 35 days *in vitro*. The average values per electrode are shown as Tukey box plots (middle line denotes the median). The cultures showed increasing spontaneous electrical activity up to four weeks in culture. Burst duration increased until DIV20, after which it started to decrease and stabilize (n = 23). **D)** Phosphorylation of TrkB, ERK1 and ERK2 15 min after BDNF (20 ng/ml) treatment at DIV14 and DIV35. Graphs show means ± S.D. *p < 0.05, **p < 0.01, ***p < 0.001, Welsch *t*-test (western blot). n = 4–6 per group.

anti-ERK1/2 (#9102, 1:1000, CST). The membranes were washed in Tris-buffered saline with 0.1% Tween (TBST) and incubated with horseradish peroxidase-conjugated secondary antibodies (1:10000 in non-fat dry milk, 1 h at RT; Bio-Rad). After subsequent TBST washes, secondary antibodies were visualized using enhanced chemiluminescence (ECL Plus™, ThermoScientific, Vantaa, Finland) for detection by Biorad ChemiDoc™ MP camera (Bio-Rad Laboratories, Helsinki, Finland). Densitometric analysis of the chemiluminescent blots were quantified using ImageJ software (ImageJ 1.46v, National Institute of Health, USA). The phospho-proteins of each sample were normalized to their respective total proteins, and the results are shown as percentage of control average. The samples from wells that were excluded from MEA analysis (see section 2.5) were also excluded from western blot analyses.

2.7. Statistical analysis

Statistical analyses and graphs were prepared using GraphPad Prism software (v. 9) (GraphPad Software, San Diego CA, USA). Mann–Whitney *U* test was performed for the electrophysiological data due to the non-normal distribution of the measured parameters. For western blot results, two-tailed independent Welch *t*-test was used when comparing two treatment groups. One-way ANOVA with Dunnett's post hoc was used when there were more than two study groups in the experiment. A p-value under 0.05 was considered significant in all tests. Details of statistical tests are shown in Tables S1 and S2 for western blot and electrophysiological experiments, respectively.

3. Results

3.1. Morphological, electrophysiological and biochemical characteristics of the cultures

To first characterize the morphological and functional properties and their development in the rat cortical neuron cultures across time, cultures were followed for 35 days. The cultures grown on coverslips formed neuronal networks with increasing complexity over time, as indicated by MAP2- and β3-tubulin-positive cells connected with synapses (SYN) (Fig. 2A). The cultures also contained spontaneous astrocytes that expressed common astrocyte markers GFAP and S100β (Fig. 2A). The cultures grown on mw-MEA plates visually appear to be similar and show similar morphological behavior that increases in complexity over maturation as shown by phase contrast images at different time points (Fig. 2B, Fig. S1A for DIV35). From DIV8 onward, the neurons started to develop spiking and bursting activity that rapidly increased at the end of the second week *in vitro*, as shown by increasing spike and burst rates (Fig. 2C) as well the growing number of active electrodes (Fig. S1B). The steady rise in spike and burst rate continued until the end of the fourth week *in vitro* (Fig. 2C). After this, the activity started to gradually decline (Fig. 2C). Burst duration rose until DIV18, after which it stabilized to shorter durations (Fig. 2C), which is typically observed in primary neuronal cultures (Wagenaar et al., 2006a). Furthermore, neuronal network connectivity, evaluated by synchronized bursting across the twelve electrodes, followed similar patterns as the bursting activity (Fig. S1C).

In order to characterize the responsiveness of the cultures to BDNF (Antila et al., 2014), we acutely applied BDNF at DIV14 and DIV35 and analyzed its effects at biochemical level. Specifically, the phosphorylation of $TrkB^{816}$, which is associated with activation of intracellular PLCγ pathway, as well phosphorylation of its other downstream effectors, ERK1 and ERK2, were assessed. BDNF caused rapid and robust upregulation in phosphorylated TrkB (*p*-TrkB) and ERK1/2 (*p*-ERK1/2) at DIV14 cultures (Fig. 2D; $p = 0.002$, $p = 0.0008$ and $p = 0.0057$, respectively). In DIV35 cultures the upregulation of phosphorylation in TrkB and ERK1/2 was also observed ($p = 0.002$, $p = 0.0016$, $p = 0.0226$, respectively), but the effect size was more modest than at DIV14 (Fig. 2D). We also measured the effects of BDNF on neuronal activity in mw-MEA but any obvious effects on spiking, bursting or burst duration were not observed at neither DIV14 nor DIV35 (Figs. S2A–B).

3.2. The electrophysiological and biochemical responsiveness of neuronal cultures to pharmacological stimulation and inhibition on mw-MEAs

Obtained biochemical and electrophysiological data, and previous observations (Lepack et al., 2015, 2016), guided us to select DIV14 culture for further studies. Because the balance between excitation and inhibition is governed by glutamatergic and GABAergic neurons, we performed immunocytochemical analysis at this time point to verify the presence of GABAergic neurons in the cultures. The relative number of GABAergic neurons at DIV14 was quantified based on immunofluorescent images (Fig. 3A). Approximately 10% of all neurons were GABA positive, indicating an existing GABAergic system in the cultures (Fig. 3B).

To characterize the sensitivity of the cultures to pharmacologically induced neuronal stimulation and inhibition and to study its correlation with TrkB and ERK1/2 phosphorylation, we treated the cultures with carbachol or diazepam. Carbachol is a mixed cholinergic agonist that has been previously shown to evoke neuronal activity *in vitro* (Kilb and Luhmann, 2003; Tateno et al., 2005), whereas diazepam is a benzodiazepine that potentiates the effects of endogenous GABA on $GABA_A$ ion channel receptor resulting in inhibition in mature neurons (Khalilov et al., 1999; Serafini et al., 1998; Twyman et al., 1989). One group of cultures were treated with carbachol for the whole 30 min recording time (CC), whereas a subset of wells were first exposed to carbachol for 15 min, after which diazepam was added to the wells for the remaining 15 min of recording (CC + DZ). Example traces of one representative electrode from a well in CC + DZ group is shown in Fig. 3C, which demonstrates a visible increase in activity from baseline upon carbachol treatment. When diazepam was added to the same well, the activity was immediately abolished, overriding the carbachol-induced increases in activity, as shown by the complete disappearance of spikes and bursts from the electrode (Fig. 3C). Raster plot (Figure S3A) shows activity at a level of a single well, demonstrating that the stimulating effect of carbachol and silencing effect of diazepam are network-level phenomena influencing neurons on the whole electrode area. Notably, GABA is a depolarizing neurotransmitter early in the development, but turns into hyperpolarizing during maturation of neurons *in vivo* as well as in culture (Ben-Ari et al., 2007; Rivera et al., 1999). The prominent silencing effect of diazepam that potentiates the effects of GABA suggests that at DIV14, GABA shift from depolarizing to hyperpolarizing has already largely occurred in our cultures.

Quantification of the effects across all cultures showed that carbachol and diazepam produced consistent effects on the cortical networks. Whereas the number of active electrodes tended to increase from the baseline in control group (+15% on average), carbachol treatment caused a 29% decrease in the number of active electrodes from the baseline ($p = 0.0007$ control vs. CC) (Fig. 3D). Diazepam essentially abolished the activity in all electrodes (Figure S3A) in each well (Figure S3B), as indicated by 100% drop in active electrodes compared to baseline (Fig. 3D). In the complete absence of remaining active electrodes, further analysis of the spiking and bursting characteristics during diazepam stimulation was not applicable (N.A.; Figure S3A-B) and thus these were only quantified for control and carbachol treatments. Carbachol increased neuronal spiking on average by 2.3-fold compared to control ($p = 0.0007$) (Fig. 3E, S3B). Bursting was also increased by 2.9-fold compared to control cultures ($p = 0.0027$) (Fig. 3E, S3B). Carbachol also caused 40% increase in burst duration ($p = 0.0080$), which was associated with significantly decreased number (0.49-fold) and rate (0.67-fold) of spikes per burst ($p = 0.0007$ for both) compared to control (Fig. 3E, S3B). Percentage of all spikes occurring in bursts decreased to under half of control during carbachol treatment ($p = 0.0007$) (Fig. 3E, S3B). The interburst interval showed variable

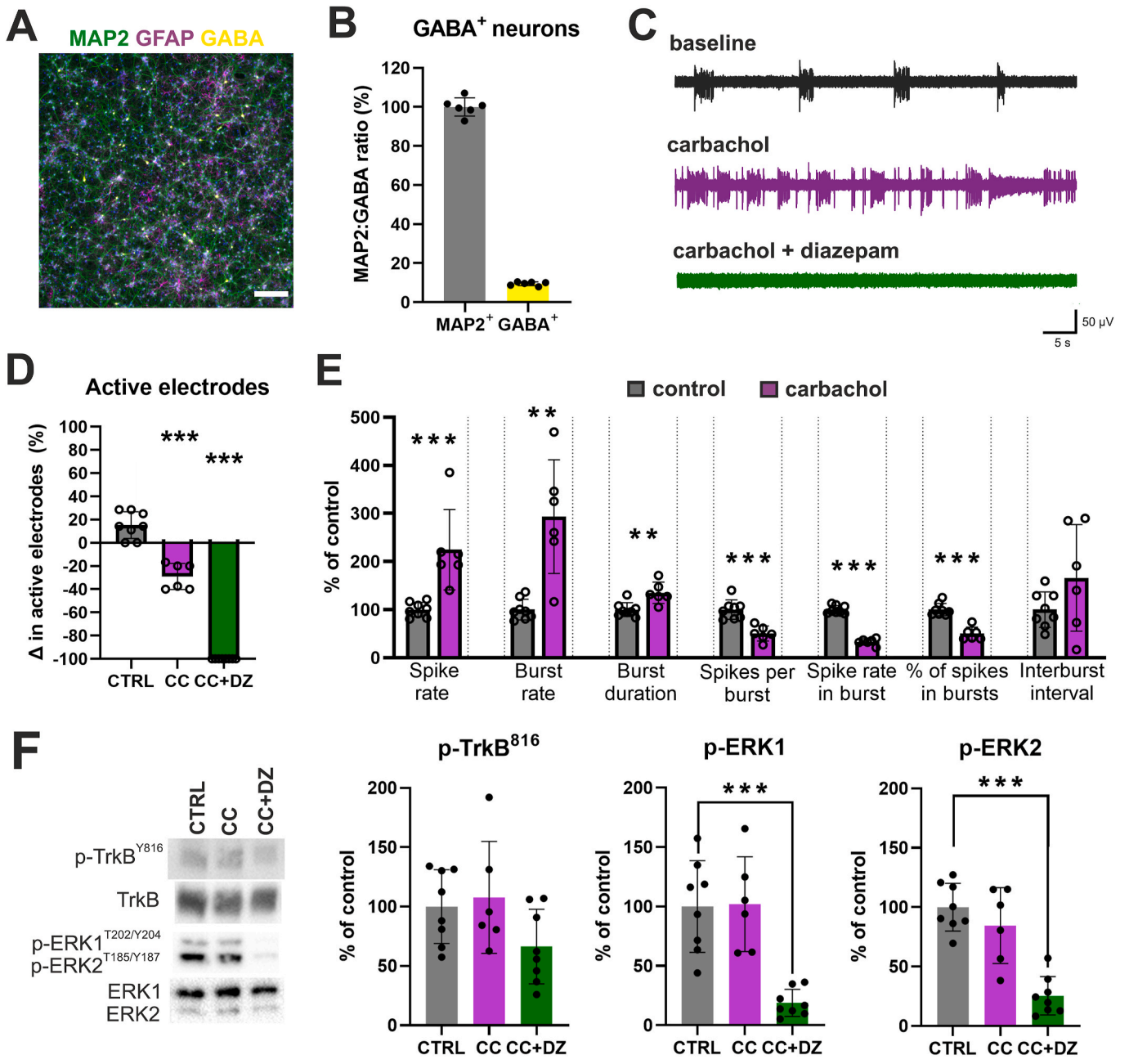

Fig. 3. TrkB and ERK1/2 phosphorylation and MEA activity after treatment with carbachol (25 µM) and diazepam (10 µM). A) Immunocytochemical (ICC) staining showing GABA-positive neurons in the culture at DIV14. The scale bar is 200 µm **B)** The percentage of GABA-positive neurons in the DIV14 culture was characterized based on the ICC (n = 6). **C)** Representative images of activity signals in a single electrode during baseline spontaneous electrical activity (black), during carbachol stimulation (purple) and after application of diazepam (green) to the same culture. **D)** The number of active electrodes tend to increase from baseline in the control cultures, whereas carbachol (CC) decreased the number of active electrodes. Application of diazepam (DZ) to the culture media completely abolished the number or active electrodes in all the tested wells. **E)** Carbachol evoked increased spiking and bursting in active electrodes, and increased burst duration. The number and rate of spikes within the bursts decreased, as well the percentage of spikes occurring in bursts. The effects on interburst interval were variable. **F)** *p*-TrkB and *p*-ERK1/2 at DIV14 30 min after treatment with carbachol (CC) or carbachol + diazepam (CC + DZ). Diazepam strongly downregulated *p*-ERK1 and *p*-ERK2, while *p*-TrkB was relatively unchanged. Carbachol did not affect phosphorylation of TrkB or ERK1/2. The graphs show means ± S.D.**$p < 0.01$, ***$p < 0.001$, Mann-Whitney *U* test (electrophysiological data) or one-way ANOVA (western blot). n = 6–8 per group.

changes after carbachol ($p > 0.05$). Additionally, the analysis of simultaneously occurring bursts showed that the bursts during carbachol treatment were less synchronous than in the respective control wells ($p < 0.0001$) (Fig. S3C). Hence, carbachol induced increased spiking and bursting activity in neurons while decreased network synchronicity.

In order to test whether the increases and decreases in activity were associated with biochemical changes in BDNF signaling cascade, western blot analyses were performed from the samples collected from the same cultures immediately after MEA recording. Carbachol did not affect the levels of phosphorylated TrkB or ERK1/2 ($p > 0.05$), indicating that increased network activity elicited by carbachol stimulation was not accompanied by changes in BDNF-associated targets (Fig. 3F). On the contrary, while the silencing effect of diazepam was accompanied by a negligible change in *p*-TrkB ($p > 0.05$), the phosphorylation of ERK1 and ERK2 was significantly downregulated compared to control

($p < 0.0001$ for ERK1 and ERK2) (Fig. 3F).

3.3. Concentration-dependent effects of ketamine on electrophysiological network activity and TrkB and ERK1/2 signaling

We next studied the effects of ketamine on DIV14 neuronal cultures. Ketamine has previously been reported to elicit biochemical effects with a bell-shaped concentration-response curve in a cortical neuron culture (Lepack et al., 2016). We chose to probe for the effects of low, sub-micromolar (100–500 nM) as well as a high (10 μM) concentrations, in accordance with Lepack and colleagues.

Representative images of electrophysiological activity during 100 nM-10 μM ketamine and their respective controls are shown at the level of a single electrode and a single well in Fig. 4A and Fig. S4A, respectively. The effects on the spiking and bursting parameters are shown in Fig. 4B–I (absolute values presented in Fig. S4B). The high concentration (10 μM) of ketamine caused prominent inhibition of the network activity. Compared to control wells, the spiking activity was decreased 60–70% ($p = 0.0025$), which was accompanied by a decrease in the number of active electrodes from the baseline (−16% versus 2% increase in control, $p = 0.0025$). High ketamine concentration also reduced burst rate (34% decrease, $p = 0.0177$), and other burst characteristics such as burst duration, number of spikes per burst and the percentage of all spikes occurring in bursts when compared to control ($p = 0.0025$, $p = 0.0025$ and $p = 0.0480$, respectively). Interestingly, spike rate in bursts increased 1.4-folds compared to control ($p = 0.0025$). At 500 nM, ketamine significantly decreased neuronal spiking (spikes/min) and the number of spikes in bursts (74% of control, $p = 0.0062$, and 73% of control, $p = 0.0031$, respectively). The number of active electrodes as well as burst rate, burst duration, spike rate in bursts, percentage of spikes in bursts, and interburst interval remained relatively unchanged ($p > 0.05$). Lower concentrations of ketamine (100 and 250 nM) did not cause significant changes in neuronal electrophysiological activity (Fig. 4, S4A-B, $p > 0.05$ for all) compared to their respective control cultures. To further study the effects on burst synchronization, simultaneous bursts were quantified. During 10 μM ketamine treatment, bursts occurred on average on 4.4 electrodes simultaneously, whereas the value was approximately 5.5 in their respective control cultures ($p = 0.0215$). Lower concentrations of ketamine (100–500 nM) did not differ from their control cultures in burst synchronicity ($p > 0.05$) (Fig. S4C).

The phosphorylation of TrkB and ERK1/2 were measured from the cultures lysed immediately after the 15-min MEA recording. The low concentrations of ketamine (100, 250 or 500 nM) did not affect the levels of phosphorylated TrkB or ERK1/2 ($p > 0.05$) (Fig. 4J). However, high concentration (10 μM) of ketamine caused a significant decrease in ERK1 and ERK2 phosphorylation ($p = 0.0001$ and $p = 0.0012$, respectively), while TrkB phosphorylation remained unaltered ($p > 0.05$) (Fig. 4J).

4. Discussion

Activation of TrkB receptors and ERK1/2 signaling have been intimately connected to antidepressant effects of subanesthetic-dose ketamine and its enantiomers *in vivo* (Lepack et al., 2015; Li et al., 2010; Liu et al., 2012; Yang et al., 2015, 2018). These biochemical events may be triggered via increased neuronal activity through disinhibition of GABAergic interneurons (Zanos et al., 2018). In this study, we combined multiwell-MEA (mw-MEA) recordings with western blot analyses to test whether sub-micromolar racemic ketamine induces network activity accompanied with increased TrkB-ERK1/2 signaling in primary cortical neurons. Opposite effects were expected to be observed with high ketamine concentration. To first characterize our cultures, we showed that neurons exhibited typical development of spontaneous electrical activity during maturation (Enright et al., 2020; Hyvärinen et al., 2019; Wagenaar et al., 2006a). Stimulation and inhibition of network activity could be produced by applying carbachol and diazepam to the cultures, respectively, showing that electrical neuronal network activity could be pharmacologically shifted to either direction. These effects are in line with previous reports describing desynchronizing and stimulating effects of carbachol (Tateno et al., 2005) and robust inactivation of network activity with diazepam (McConnell et al., 2012) in cultures. Interestingly, carbachol decreased the number of active electrodes while prominently increasing and desynchronizing activity in the electrodes remaining active, verified as decreased synchronicity in bursts, elucidating the tight interplay of the neurons within the network. Diazepam is a positive allosteric modulator of $GABA_A$ receptors and requires the release of endogenous GABA to elicit its effects (Twyman et al., 1989). The immediate, almost complete cessation of activity after application of diazepam demonstrates the presence of spontaneously active inhibitory GABAergic system in these networks. Indeed, functional inhibitory GABAergic system is needed to uncover effects brought about via disinhibitory mechanism, which is proposedly important for ketamine's effects (Zanos et al., 2018).

Ketamine induced a concentration-dependent decrease in neuronal electrical activity on mw-MEAs. The high 10 μM concentration of ketamine caused prominent inhibition of spiking and decreased the number of active electrodes. This result was expected based on ketamine's affinity to block the excitatory NMDARs with an inhibitory constant of ~1 μM in cells (Dravid et al., 2007; Gilling et al., 2009; Kotermanski and Johnson, 2009; Parsons et al., 1995). The silencing effect of high ketamine concentrations on spiking have also been recapitulated in a few previous MEA studies *in vitro* (Belle et al., 2018; Hondebrink et al., 2017; McConnell et al., 2012). Our results show that 10 μM ketamine also decreases the burst rate and reduces their duration, which is associated with reduced number of spikes per burst as well as increased average spike rate within the bursts. Unexpectedly, the effect of 500 nM ketamine was already inhibiting the spiking, whereas burst characteristics, other than the number of spikes per burst, were relatively unaffected. The lower concentrations of ketamine did not affect spike or burst rate or other burst properties. These results are in accordance with a previous MEA study, that also studied the effects of sub-micromolar concentrations of ketamine on spiking activity and observed a dose-dependent linear decrease in mean spiking rate (IC_{50} of 1.2 μM), without increases in spiking at any concentration (Hondebrink et al., 2017). We and Hondebrink et al. (2017) considered the pooled activity of all neurons without sorting them to putative pyramidal neurons and interneurons. Concomitant increase in firing of pyramidal neurons and decrease in the firing of interneurons, as hypothesized to occur during disinhibition, could counteract each other when the pooled average activity of unclassified neuron types is considered. However, as the ratio of GABAergic neurons to all neurons in the cultures was relatively low, this is unlikely to completely mask the effect in this study. Collectively these studies indicate that ketamine concentration-dependently reduces neuronal network activity in culture, perhaps reflecting the clinical anesthetic actions of ketamine in animals and humans at high dose. The hypothesized increase in activity with sub-micromolar concentrations of ketamine was not observed. However, there are also *in vivo* studies that have not measured any increases, only decreases, in cortical pyramidal neuron firing with ketamine (Amat-Foraster et al., 2018; Shen et al., 2018). Some studies have also indicated that low-dose ketamine would exhibit disinhibition of the cortex through thalamus, not via local cortical interneurons, which would not be seen in a cortical neuron culture (Amat-Foraster et al., 2019). Moreover, the extracellular concentrations of ketamine in the brain after its systemic administration in rodents – or humans - is hard to precisely estimate, further complicating the translation of *in vivo* to *in vitro* results. Thus, it is possible that the brain concentrations that are relevant to antidepressant effects are even lower than those tested here.

BDNF induced prominent TrkB and ERK1/2 phosphorylation in our cultures at DIV14, demonstrating that neurons readily respond to BDNF at this maturation point and thus the phosphorylation of these proteins serves as a biochemical marker of BDNF release. As BDNF release is

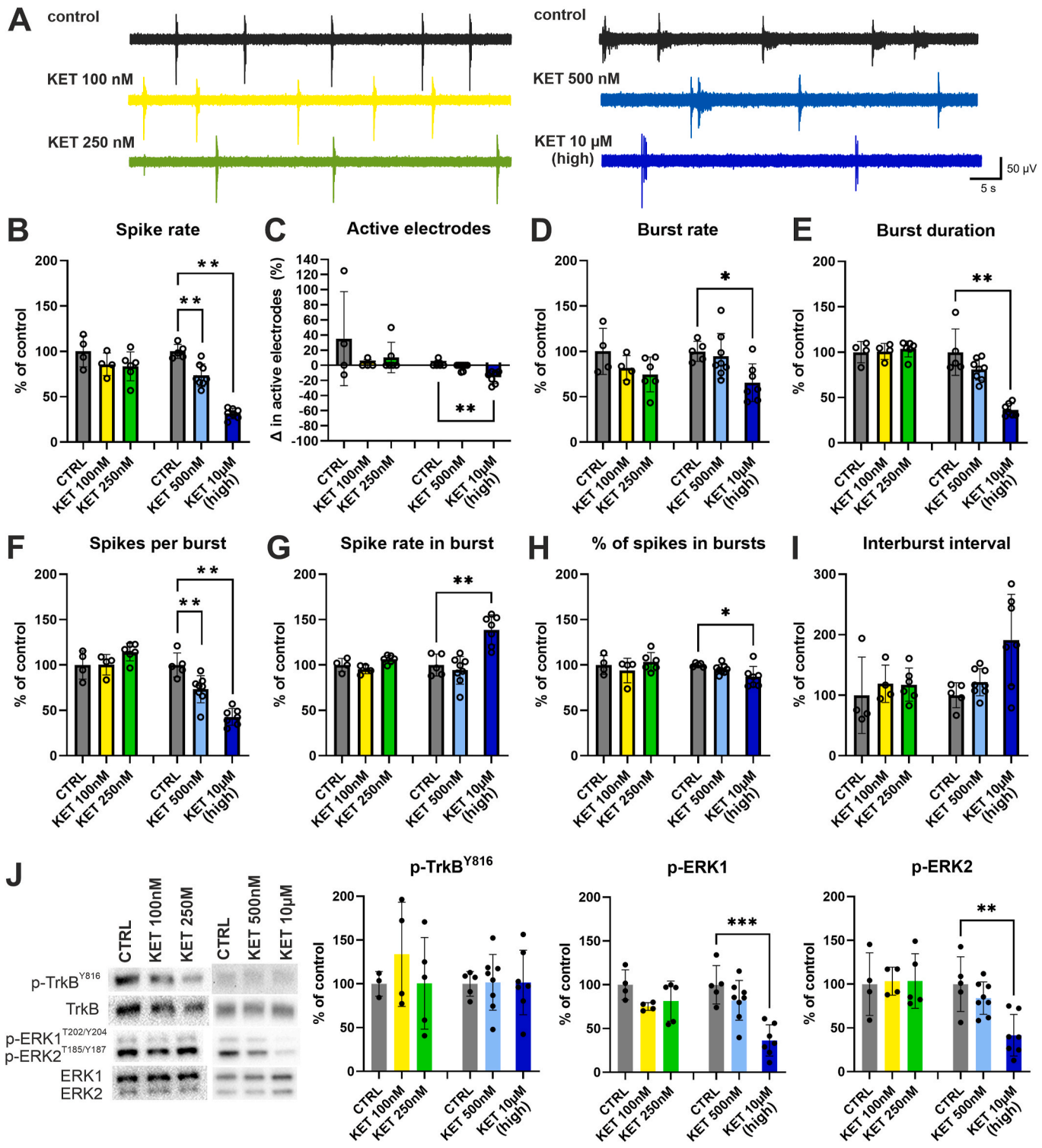

Fig. 4. Concentration-dependent effects of ketamine on MEA activity and TrkB and ERK1/2 signaling. A) Representative MEA electrode signals of DIV14 cultures treated with different concentrations of ketamine (KET) or their respective controls. **B)** The lowest tested concentrations (100–250 nM) of KET did not influence neuronal spiking, whereas dose-dependent decrease on spike rate was observed at 500 nM and high 10 µM concentration ketamine. **C)** The number of active electrodes decreased after treating cultures with 10 µM KET. **D)** High KET concentration (10 µM) decreased neuronal burst rate, whereas other concentrations showed negligible effects. **E)** The duration of bursts was significantly shortened by 10 µM KET, whereas the lower concentrations did not affect the duration of bursts. **F)** The number of spikes per burst was decreased by 500 nM and 10 µM KET. **G)** Spike rate in bursts was increased by 10 µM KET, whereas the lower concentrations were comparable to control treatment. **H)** The percentage of spikes in bursts was decreased after 10 µM KET. **I)** The interburst interval was not significantly affected by any concentration of KET. **J)** *p*-TrkB and *p*-ERK1/2 after 15-min treatment with KET. Phosphorylation of TrkB was comparable to control in all concentration levels of KET. Phosphorylation of ERK1 and ERK2 were significantly reduced by 10 µM KET. The lower concentrations did not influence phosphorylation of ERK1/2. The graphs show means ± S.D. *p < 0.05, **p < 0.01, ***p < 0.001, Mann-Whitney *U* test (electrophysiological data) or one-way ANOVA (western blot). n = 4–8 per group.

suggested to be activity-dependent, the high neuronal network activity induced by carbachol was expected to increase TrkB and ERK1/2 signaling. However, carbachol had negligible effects on both TrkB and ERK1/2 phosphorylation. On the contrary, the diazepam-induced silencing of the cultures was associated with downregulation of *p*-ERK1/2, which was not however accompanied with changes in TrkB phosphorylation. This phenomenon was also recapitulated with high concentration of ketamine that strongly inhibited network activity. The low concentrations of ketamine that were either associated with no effect (100 and 250 nM) or slight activity-reducing effect (500 nM) did not alter *p*-TrkB or *p*-ERK1/2 levels. These results are contradictory to those by Lepack et al. (2015, 2016), where these concentrations were reported to induce BDNF release and increase *p*-ERK levels, with 500 nM showing the peak effects already in 15 min. These effects were suggested to be caused by increased electrical activity, based on that AMPAR antagonist NBQX abolished the signaling (Lepack et al., 2015, 2016). In this study we did not detect an increase, but a decrease in electrical activity with 500 nM ketamine, and further, our carbachol results contradict the hypothesis of a direct relationship between increased activity and TrkB-ERK1/2 signaling. Notably, NBQX that was used in the studies by Lepack et al. (2015, 2016), could hinder the depolarization-induced relief of Mg^{2+} blockade in NMDAR channels. As this is required for an open channel NMDAR blocker like ketamine for accessing its binding site, NBQX could inhibit the downstream effects initiated by any NMDAR-dependent mechanism. Interestingly, previous studies suggest that (R)-ketamine, which has lower potency to block NMDARs compared to (S)-ketamine, more robustly regulates ERK1/2 signaling in the adult brain (Yang et al., 2018). ERK inhibitor also abolished the antidepressant-like effects of (R)- but not (S)-ketamine, implying mechanistic differences between the enantiomers.

Maturity of the cultures affects the network properties and expression of receptors, including different NMDAR subtypes and other targets of ketamine, as well as BDNF-TrkB signaling (Sava et al., 2012; Wagenaar et al., 2006a; Zhou et al., 2011). We studied the effects of pharmacological treatments at DIV14, where the cultures are relatively immature and the neuronal circuits are still being refined. Notably, Lepack et al. (2015, 2016) used even more immature cultures (DIV10). In contrast, *in vivo* studies supporting disinhibition mechanism of ketamine are done on adult rodents (Ali et al., 2020; Gerhard et al., 2020; Homayoun and Moghaddam, 2007). The different level of maturation (Jin et al., 2013) as well as cellular complexity could explain the differences between *in vitro* and *in vivo* studies. In our cultures at DIV14, approximately 10% of all cells were astrocytes (Ahtiainen et al., 2021) and approximately 10% of neurons were GABAergic. In adult rodent and primate cortex, the ratios of GABAergic neurons and astrocytes to all neurons are higher (Hendry et al., 1987; Herculano-Houzel, 2014; Markram et al., 2004). The different ratios between GABAergic and glutamatergic neurons may result in different balance between excitatory and inhibitory neurotransmission in the cultures and hence affect the response of networks to ketamine. Moreover, the amount of astrocytes may also be important since their number has been shown to affect the electrophysiological responses to drugs in culture (Ahtiainen et al., 2021; Enright et al., 2020) and they have been implicated in the mechanism of action of ketamine (Stenovec et al., 2021). Furthermore, as the primary cultures contain very small amounts of microglia (Enright et al., 2020), it is worth noting that ketamine, specifically its (R)-enantiomer, has been shown to increase ERK phosphorylation in cultured microglia in concentration-dependent manner (Yao et al., 2022). Thus, ketamine and its enantiomers can have different effects and/or mechanisms depending on cell type.

In conclusion, this study utilizes multiwell-MEA platform enabling several parallel samples for electrophysiological assessment coupled with biochemical assays to elucidate the relationship between electrophysiological activity and TrkB-ERK1/2 signaling in cortical neuron cultures exposed to ketamine. We found that the inhibition of network activity is associated with reduction on ERK1/2 phosphorylation, and this can be readily detected with high concentration of ketamine. However, we did not observe the hypothesized increase in neuronal network activity and TrkB-ERK1/2 phosphorylation at sub-micromolar ketamine concentrations. In future studies, it would be interesting to study the concentration-dependent effects of ketamine's enantiomers in similar experimental settings in primary cell cultures comprising of neurons and astrocytes, or microglia, at different stages of maturation.

Funding

The works of J.M.A.T and A.A was supported by the Jane and Aatos Erkko Foundation, Helsinki, Finland, project "Biological Neuronal Communications and Computing with ICT" and the European Union's Horizon 2020 Research and Innovation Programme under grant agreement No. 824164, project "Hybrid Enhanced Regenerative Medicine Systems". Otherwise, this research did not receive any specific grant from funding agencies in the public, commercial, or not-for-profit sectors. T.R. and S.K. have received grants from the Sigrid Jusélius Foundation.

Author contributions

A.A. and I.A. contributed equally to this work. Conceptualization: T. R., S.K., M.R., I.A., A.A. and J.M.A.T; Data curation: A.A., I.A.; Formal analysis: A.A, I.A. and M.R.; Funding acquisition: J.M.A.T., A.A., J.H., and T.R.; Investigation: A.A, I.A. and M.R; Methodology: T.R., J.M.A.T., and A.A.; Project administration: T.R., J.H., M.R., I.A. and A.A; Resources: J.H., T.R.; Software: A.A., J.M.A.T; Supervision: T.R., J.H. and J.M.A.T; Validation: T.R., J.H., S.K., M.R., I.A. and A.A.; Visualization: I. A., A.A.; Writing - original draft: I.A., A.A.; Writing - review & editing: T. R., J.H., S.K., J.M.A.T., M.R., I.A., and A.A.

Declaration of competing interest

The authors declare no conflict of interest.

Data availability

Data will be made available on request.

Acknowledgements

The authors acknowledge Dr. Stanislav Rozov and statistician Heini Huhtala for comments on the data processing and statistical analysis.

Appendix A. Supplementary data

Supplementary data to this article can be found online at https://doi.org/10.1016/j.neuropharm.2023.109481.

References

Ahtiainen, A., Genocchi, B., Tanskanen, J.M.A., Barros, M.T., Hyttinen, J.A.K., Lenk, K., 2021. Astrocytes exhibit a protective role in neuronal firing patterns under chemically induced seizures in neuron–astrocyte Co-cultures. IJMS 22, 12770. https://doi.org/10.3390/ijms222312770.

Ali, F., Gerhard, D.M., Sweasy, K., Pothula, S., Pittenger, C., Duman, R.S., Kwan, A.C., 2020. Ketamine disinhibits dendrites and enhances calcium signals in prefrontal dendritic spines. Nat. Commun. 11, 72. https://doi.org/10.1038/s41467-019-13809-8.

Amat-Foraster, M., Celada, P., Richter, U., Jensen, A.A., Plath, N., Artigas, F., Herrik, K. F., 2019. Modulation of thalamo-cortical activity by the NMDA receptor antagonists ketamine and phencyclidine in the awake freely-moving rat. Neuropharmacology 158, 107745. https://doi.org/10.1016/j.neuropharm.2019.107745.

Amat-Foraster, M., Jensen, A.A., Plath, N., Herrik, K.F., Celada, P., Artigas, F., 2018. Temporally dissociable effects of ketamine on neuronal discharge and gamma oscillations in rat thalamo-cortical networks. Neuropharmacology 137, 13–23. https://doi.org/10.1016/j.neuropharm.2018.04.022.

Antila, H., Autio, H., Turunen, L., Harju, K., Tammela, P., Wennerberg, K., Yli-Kauhaluoma, J., Huttunen, H.J., Castrén, E., Rantamäki, T., 2014. Utilization of in

situ ELISA method for examining Trk receptor phosphorylation in cultured cells. J. Neurosci. Methods 222, 142–146. https://doi.org/10.1016/j.jneumeth.2013.11.001.

Autry, A.E., Adachi, M., Nosyreva, E., Na, E.S., Los, M.F., Cheng, P., Kavalali, E.T., Monteggia, L.M., 2011. NMDA receptor blockade at rest triggers rapid behavioural antidepressant responses. Nature 475, 91–95. https://doi.org/10.1038/nature10130.

Belle, A.M., Enright, H.A., Sales, A.P., Kulp, K., Osburn, J., Kuhn, E.A., Fischer, N.O., Wheeler, E.K., 2018. Evaluation of in vitro neuronal platforms as surrogates for in vivo whole brain systems. Sci. Rep. 8, 10820 https://doi.org/10.1038/s41598-018-28950-5.

Ben-Ari, Y., Gaiarsa, J.-L., Tyzio, R., Khazipov, R., 2007. GABA: a pioneer transmitter that excites immature neurons and generates primitive oscillations. Physiol. Rev. 87, 1215–1284. https://doi.org/10.1152/physrev.00017.2006.

Casarotto, P.C., Girych, M., Fred, S.M., Kovaleva, V., Moliner, R., Enkavi, G., Biojone, C., Cannarozzo, C., Sahu, M.P., Kaurinkoski, K., Brunello, C.A., Steinzeig, A., Winkel, F., Patil, S., Vestring, S., Serchov, T., Diniz, C.R.A.F., Laukkanen, L., Cardon, I., Antila, H., Rog, T., Piepponen, T.P., Bramham, C.R., Normann, C., Lauri, S.E., Saarma, M., Vattulainen, I., Castrén, E., 2021. Antidepressant drugs act by directly binding to TRKB neurotrophin receptors. Cell 184, 1299–1313.e19. https://doi.org/10.1016/j.cell.2021.01.034.

Castrén, E., Võikar, V., Rantamäki, T., 2007. Role of neurotrophic factors in depression. Curr. Opin. Pharmacol. 7, 18–21. https://doi.org/10.1016/j.coph.2006.08.009.

de la Salle, S., Choueiry, J., Shah, D., Bowers, H., McIntosh, J., Ilivitsky, V., Knott, V., 2016. Effects of ketamine on resting-state EEG activity and their relationship to perceptual/dissociative symptoms in healthy humans. Front. Pharmacol. 7.

Dravid, S.M., Erreger, K., Yuan, H., Nicholson, K., Le, P., Lyuboslavsky, P., Almonte, A., Murray, E., Mosley, C., Barber, J., French, A., Balster, R., Murray, T.F., Traynelis, S. F., 2007. Subunit-specific mechanisms and proton sensitivity of NMDA receptor channel block: proton sensitivity of NMDA receptor channel blockers. J. Physiol. 581, 107–128. https://doi.org/10.1113/jphysiol.2006.124958.

Duman, R.S., Deyama, S., Fogaça, M.V., 2021. Role of BDNF in the pathophysiology and treatment of depression: activity-dependent effects distinguish rapid-acting antidepressants. Eur. J. Neurosci. 53, 126–139. https://doi.org/10.1111/ejn.14630.

Enright, H.A., Lam, D., Sebastian, A., Sales, A.P., Cadena, J., Hum, N.R., Osburn, J.J., Peters, S.K.G., Petkus, B., Soscia, D.A., Kulp, K.S., Loots, G.G., Wheeler, E.K., Fischer, N.O., 2020. Functional and transcriptional characterization of complex neuronal co-cultures. Sci. Rep. 10, 11007 https://doi.org/10.1038/s41598-020-67691-2.

Gerhard, D.M., Pothula, S., Liu, R.-J., Wu, M., Li, X.-Y., Girgenti, M.J., Taylor, S.R., Duman, C.H., Delpire, E., Picciotto, M., Wohleb, E.S., Duman, R.S., 2020. GABA interneurons are the cellular trigger for ketamine's rapid antidepressant actions. J. Clin. Invest. 130, 1336–1349. https://doi.org/10.1172/JCI130808.

Gilling, K.E., Jatzke, C., Hechenberger, M., Parsons, C.G., 2009. Potency, voltage-dependency, agonist concentration-dependency, blocking kinetics and partial untrapping of the uncompetitive N-methyl-d-aspartate (NMDA) channel blocker memantine at human NMDA (GluN1/GluN2A) receptors. Neuropharmacology 56, 866–875. https://doi.org/10.1016/j.neuropharm.2009.01.012.

Hendry, S., Schwark, H., Jones, E., Yan, J., 1987. Numbers and proportions of GABA-immunoreactive neurons in different areas of monkey cerebral cortex. J. Neurosci. 7, 1503–1519. https://doi.org/10.1523/JNEUROSCI.07-05-01503.1987.

Herculano-Houzel, S., 2014. The glia/neuron ratio: how it varies uniformly across brain structures and species and what that means for brain physiology and evolution: the Glia/Neuron Ratio. Glia 62, 1377–1391. https://doi.org/10.1002/glia.22683.

Homayoun, H., Moghaddam, B., 2007. NMDA receptor hypofunction produces opposite effects on prefrontal cortex interneurons and pyramidal neurons. J. Neurosci. 27, 11496–11500. https://doi.org/10.1523/JNEUROSCI.2213-07.2007.

Hondebrink, L., Kasteel, E.E.J., Tukker, A.M., Wijnolts, F.M.J., Verboven, A.H.A., Westerink, R.H.S., 2017. Neuropharmacological characterization of the new psychoactive substance methoxetamine. Neuropharmacology 123, 1–9. https://doi.org/10.1016/j.neuropharm.2017.04.035.

Hyvärinen, T., Hyysalo, A., Kapucu, F.E., Aarnos, L., Vinogradov, A., Eglen, S.J., Ylä-Outinen, L., Narkilahti, S., 2019. Functional characterization of human pluripotent stem cell-derived cortical networks differentiated on laminin-521 substrate: comparison to rat cortical cultures. Sci. Rep. 9, 17125 https://doi.org/10.1038/s41598-019-53647-8.

Jin, J., Gong, K., Zou, X., Wang, R., Lin, Q., Chen, J., 2013. The blockade of NMDA receptor ion channels by ketamine is enhanced in developing rat cortical neurons. Neurosci. Lett. 539, 11–15. https://doi.org/10.1016/j.neulet.2013.01.034.

Khalilov, I., Dzhala, V., Ben-Ari, Y., Khazipov, R., 1999. Dual role of GABA in the neonatal rat Hippocampus. DNE 21, 310–319. https://doi.org/10.1159/000017380.

Kilb, W., Luhmann, H.J., 2003. Carbachol-induced network oscillations in the intact cerebral cortex of the newborn rat. Cerebr. Cortex 13, 409–421. https://doi.org/10.1093/cercor/13.4.409.

Kohtala, S., 2021. Ketamine—50 years in use: from anesthesia to rapid antidepressant effects and neurobiological mechanisms. Pharmacol. Rep. 73, 323–345. https://doi.org/10.1007/s43440-021-00232-4.

Kohtala, S., Rantamäki, T., 2021. Rapid-acting antidepressants and the regulation of TrkB neurotrophic signalling—insights from ketamine, nitrous oxide, seizures and anaesthesia. Basic Clin. Pharmacol. Toxicol. 129, 95–103. https://doi.org/10.1111/bcpt.13598.

Kohtala, S., Theilmann, W., Rosenholm, M., Müller, H.K., Kiuru, P., Wegener, G., Yli-Kauhaluoma, J., Rantamäki, T., 2019a. Ketamine-induced regulation of TrkB-GSK3β signaling is accompanied by slow EEG oscillations and sedation but is independent of hydroxynorketamine metabolites. Neuropharmacology 157, 107684. https://doi.org/10.1016/j.neuropharm.2019.107684.

Kohtala, S., Theilmann, W., Rosenholm, M., Penna, L., Karabulut, G., Uusitalo, S., Järventausta, K., Yli-Hankala, A., Yalcin, I., Matsui, N., Wigren, H.-K., Rantamäki, T., 2019b. Cortical excitability and activation of TrkB signaling during rebound slow oscillations are critical for rapid antidepressant responses. Mol. Neurobiol. 56, 4163–4174. https://doi.org/10.1007/s12035-018-1364-6.

Kotermanski, S.E., Johnson, J.W., 2009. Mg2+ imparts NMDA receptor subtype selectivity to the alzheimer's drug memantine. J. Neurosci. 29, 2774–2779. https://doi.org/10.1523/JNEUROSCI.3703-08.2009.

Leal, G.C., Bandeira, I.D., Correia-Melo, F.S., Telles, M., Mello, R.P., Vieira, F., Lima, C.S., Jesus-Nunes, A.P., Guerreiro-Costa, L.N.F., Marback, R.F., Caliman-Fontes, A.T., Marques, B.L.S., Bezerra, M.L.O., Dias-Neto, A.L., Silva, S.S., Sampaio, A.S., Sanacora, G., Turecki, G., Loo, C., Lacerda, A.L.T., Quarantini, L.C., 2021. Intravenous arketamine for treatment-resistant depression: open-label pilot study. Eur. Arch. Psychiatr. Clin. Neurosci. 271, 577–582. https://doi.org/10.1007/s00406-020-01110-5.

Lepack, A.E., Bang, E., Lee, B., Dwyer, J.M., Duman, R.S., 2016. Fast-acting antidepressants rapidly stimulate ERK signaling and BDNF release in primary neuronal cultures. Neuropharmacology 111, 242–252. https://doi.org/10.1016/j.neuropharm.2016.09.011.

Lepack, A.E., Fuchikami, M., Dwyer, J.M., Banasr, M., Duman, R.S., 2015. BDNF release is required for the behavioral actions of ketamine. Int. J. Neuropsychopharmacol. 18 https://doi.org/10.1093/ijnp/pyu033 pyu033–pyu033.

Li, N., Lee, B., Liu, R.-J., Banasr, M., Dwyer, J.M., Iwata, M., Li, X.-Y., Aghajanian, G., Duman, R.S., 2010. mTOR-dependent synapse formation underlies the rapid antidepressant effects of NMDA antagonists. Science 329, 959–964. https://doi.org/10.1126/science.1190287.

Liu, R.-J., Lee, F.S., Li, X.-Y., Bambico, F., Duman, R.S., Aghajanian, G.K., 2012. Brain-derived neurotrophic factor Val66Met allele impairs basal and ketamine-stimulated synaptogenesis in prefrontal cortex. Biol. Psychiatr. 71, 996–1005. https://doi.org/10.1016/j.biopsych.2011.09.030.

Marcantoni, W.S., Akoumba, B.S., Wassef, M., Mayrand, J., Lai, H., Richard-Devantoy, S., Beauchamp, S., 2020. A systematic review and meta-analysis of the efficacy of intravenous ketamine infusion for treatment resistant depression: january 2009 - january 2019. J. Affect. Disord. 277, 831–841. https://doi.org/10.1016/j.jad.2020.09.007.

Markram, H., Toledo-Rodriguez, M., Wang, Y., Gupta, A., Silberberg, G., Wu, C., 2004. Interneurons of the neocortical inhibitory system. Nat. Rev. Neurosci. 5, 793–807. https://doi.org/10.1038/nrn1519.

McConnell, E.R., McClain, M.A., Ross, J., LeFew, W.R., Shafer, T.J., 2012. Evaluation of multi-well microelectrode arrays for neurotoxicity screening using a chemical training set. Neurotoxicology 33, 1048–1057. https://doi.org/10.1016/j.neuro.2012.05.001.

Miyasaka, Y., Yamamoto, N., 2021. Neuronal activity patterns regulate brain-derived neurotrophic factor expression in cortical cells via neuronal circuits. Front. Neurosci. 15, 699583 https://doi.org/10.3389/fnins.2021.699583.

Moghaddam, B., Adams, B., Verma, A., Daly, D., 1997. Activation of glutamatergic neurotransmission by ketamine: a novel step in the pathway from NMDA receptor blockade to dopaminergic and cognitive disruptions associated with the prefrontal cortex. J. Neurosci. 17, 2921–2927. https://doi.org/10.1523/JNEUROSCI.17-08-02921.1997.

Muthukumaraswamy, S.D., Shaw, A.D., Jackson, L.E., Hall, J., Moran, R., Saxena, N., 2015. Evidence that subanesthetic doses of ketamine cause sustained disruptions of NMDA and AMPA-mediated frontoparietal connectivity in humans. J. Neurosci. 35, 11694–11706. https://doi.org/10.1523/JNEUROSCI.0903-15.2015.

Nosyreva, E., Szabla, K., Autry, A.E., Ryazanov, A.G., Monteggia, L.M., Kavalali, E.T., 2013. Acute suppression of spontaneous neurotransmission drives synaptic potentiation. J. Neurosci. 33, 6990–7002. https://doi.org/10.1523/JNEUROSCI.4998-12.2013.

Park, H., Poo, M., 2013. Neurotrophin regulation of neural circuit development and function. Nat. Rev. Neurosci. 14, 7–23. https://doi.org/10.1038/nrn3379.

Parsons, C.G., Quack, G., Bresink, I., Baran, L., Przegalinski, E., Kostowski, W., Krzascik, P., Hartmann, S., Danysz, W., 1995. Comparison of the potency, kinetics and voltage-dependency of a series of uncompetitive NMDA receptor antagonists in vitro with anticonvulsive and motor impairment activity in vivo. Neuropharmacology 34, 1239–1258. https://doi.org/10.1016/0028-3908(95)00092-K.

Rivera, C., Voipio, J., Payne, J.A., Ruusuvuori, E., Lahtinen, H., Lamsa, K., Pirvola, U., Saarma, M., Kaila, K., 1999. The K+/Cl- co-transporter KCC2 renders GABA hyperpolarizing during neuronal maturation. Nature 397, 251–255. https://doi.org/10.1038/16697.

Salort, G., Álvaro-Bartolomé, M., García-Sevilla, J.A., 2019. Ketamine-induced hypnosis and neuroplasticity in mice is associated with disrupted p-MEK/p-ERK sequential activation and sustained upregulation of survival p-FADD in brain cortex: involvement of GABAA receptor. Prog. Neuro Psychopharmacol. Biol. Psychiatr. 88, 121–131. https://doi.org/10.1016/j.pnpbp.2018.07.006.

Sava, A., Formaggio, E., Carignani, C., Andreetta, F., Bettini, E., Griffante, C., 2012. NMDA-induced ERK signalling is mediated by NR2B subunit in rat cortical neurons and switches from positive to negative depending on stage of development. Neuropharmacology 62, 925–932. https://doi.org/10.1016/j.neuropharm.2011.09.025.

Serafini, R., Ma, W., Maric, D., Maric, I., Lahjouji, F., Sieghart, W., Barker, J.L., 1998. Initially expressed early rat embryonic GABAA receptor Cl– ion channels exhibit heterogeneous channel properties. Eur. J. Neurosci. 10, 1771–1783. https://doi.org/10.1046/j.1460-9568.1998.00187.x.

Shen, G., Han, F., Shi, W.-X., 2018. Effects of low doses of ketamine on pyramidal neurons in rat prefrontal cortex. Neuroscience 384, 178–187. https://doi.org/10.1016/j.neuroscience.2018.05.037.

Stenovec, M., Li, B., Verkhratsky, A., Zorec, R., 2021. Ketamine action on astrocytes provides new insights into rapid antidepressant mechanisms. Adv. Neurobiol. 26, 349–365. https://doi.org/10.1007/978-3-030-77375-5_14.

Tateno, T., Jimbo, Y., Robinson, H.P.C., 2005. Spatio-temporal cholinergic modulation in cultured networks of rat cortical neurons: spontaneous activity. Neuroscience 134, 425–437. https://doi.org/10.1016/j.neuroscience.2005.04.049.

Thoenen, H., 1995. Neurotrophins and neuronal plasticity. Science 270, 593–598. https://doi.org/10.1126/science.270.5236.593.

Thomas, C., Springer, P., Loeb, G., Berwaldnetter, Y., Okun, L., 1972. A miniature microelectrode array to monitor the bioelectric activity of cultured cells. Exp. Cell Res. 74, 61–66. https://doi.org/10.1016/0014-4827(72)90481-8.

Twyman, R.E., Rogers, C.J., Macdonald, R.L., 1989. Differential regulation of gamma-aminobutyric acid receptor channels by diazepam and phenobarbital. Ann. Neurol. 25, 213–220. https://doi.org/10.1002/ana.410250302.

Wagenaar, Daniel A., Pine, J., Potter, S.M., 2006a. An extremely rich repertoire of bursting patterns during the development of cortical cultures. BMC Neurosci. 7, 11. https://doi.org/10.1186/1471-2202-7-11.

Wagenaar, Daniel A., Nadasdy, Z., Potter, S.M., 2006b. Persistent dynamic attractors in activity patterns of cultured neuronal networks. Phys. Rev. E 73, 051907. https://doi.org/10.1103/PhysRevE.73.051907.

Yang, C., Ren, Q., Qu, Y., Zhang, J.-C., Ma, M., Dong, C., Hashimoto, K., 2018. Mechanistic target of rapamycin–independent antidepressant effects of (R)-Ketamine in a social defeat stress model. Biol. Psychiatr. 83, 18–28. https://doi.org/10.1016/j.biopsych.2017.05.016.

Yang, C., Shirayama, Y., Zhang, J., Ren, Q., Yao, W., Ma, M., Dong, C., Hashimoto, K., 2015. R-ketamine: a rapid-onset and sustained antidepressant without psychotomimetic side effects. Transl. Psychiatry 5. https://doi.org/10.1038/tp.2015.136 e632–e632.

Yao, W., Cao, Q., Luo, S., He, L., Yang, C., Chen, J., Qi, Q., Hashimoto, K., Zhang, J., 2022. Microglial ERK-NRBP1-CREB-BDNF signaling in sustained antidepressant actions of (R)-ketamine. Mol. Psychiatr. 27, 1618–1629. https://doi.org/10.1038/s41380-021-01377-7.

Ylä-Outinen, L., Tanskanen, J.M.A., Kapucu, F.E., Hyysalo, A., Hyttinen, J.A.K., Narkilahti, S., 2019. Advances in human stem cell-derived neuronal cell culturing and analysis. In: Chiappalone, M., Pasquale, V., Frega, M. (Eds.), In Vitro Neuronal Networks, Advances in Neurobiology. Springer International Publishing, Cham, pp. 299–329. https://doi.org/10.1007/978-3-030-11135-9_13.

Zanos, P., Moaddel, R., Morris, P.J., Georgiou, P., Fischell, J., Elmer, G.I., Alkondon, M., Yuan, P., Pribut, H.J., Singh, N.S., Dossou, K.S.S., Fang, Y., Huang, X.-P., Mayo, C.L., Wainer, I.W., Albuquerque, E.X., Thompson, S.M., Thomas, C.J., Zarate, C.A., Gould, T.D., 2016. NMDAR inhibition-independent antidepressant actions of ketamine metabolites. Nature 533, 481–486. https://doi.org/10.1038/nature17998.

Zanos, P., Moaddel, R., Morris, P.J., Riggs, L.M., Highland, J.N., Georgiou, P., Pereira, E.F.R., Albuquerque, E.X., Thomas, C.J., Zarate, C.A., Gould, T.D., 2018. Ketamine and ketamine metabolite pharmacology: insights into therapeutic mechanisms. Pharmacol. Rev. 70, 621–660. https://doi.org/10.1124/pr.117.015198.

Zhou, X., Xiao, H., Wang, H., 2011. Developmental changes of TrkB signaling in response to exogenous brain-derived neurotrophic factor in primary cortical neurons: developmental alteration of BDNF signaling. J. Neurochem. 119, 1205–1216. https://doi.org/10.1111/j.1471-4159.2011.07528.x.